

**NASA TECHNICAL
MEMORANDUM**

NASA TM X-52455

NASA TM X-52455

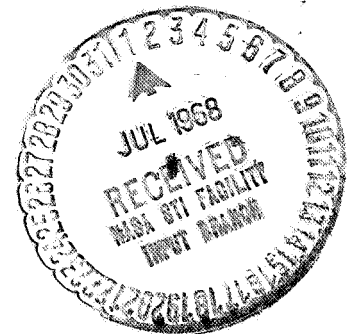
N 68-3163

FACILITY FORM 602	(ACCESSION NUMBER)	(THRU)
	(PAGES)	(CODE)
	(NASA CR OR TMX OR AD NUMBER)	(CATEGORY)

03

**OPERATING CHARACTERISTICS OF A LIQUID-COOLED
CONTAINED-ELECTROLYTE LOW-TEMPERATURE FUEL
CELL SYSTEM OVER A PERIOD OF 1500 HOURS**

by J. M. McKee, N. H. Hagedorn, and R. W. Easter
Lewis Research Center
Cleveland, Ohio



TECHNICAL PAPER proposed for presentation at
Intersociety Energy Conversion Engineering Conference
Boulder, Colorado, August 13-16, 1968

NATIONAL AERONAUTICS AND SPACE ADMINISTRATION · WASHINGTON, D.C. · 1968

**OPERATING CHARACTERISTICS OF A LIQUID-COOLED
CONTAINED-ELECTROLYTE LOW-TEMPERATURE
FUEL CELL SYSTEM OVER A PERIOD
OF 1500 HOURS**

by J. M. McKee, N. H. Hagedorn, and R. W. Easter

**Lewis Research Center
Cleveland, Ohio**

**TECHNICAL PAPER proposed for presentation at
Intersociety Energy Conversion Engineering Conference
Boulder, Colorado, August 13-16, 1968**

NATIONAL AERONAUTICS AND SPACE ADMINISTRATION

OPERATING CHARACTERISTICS OF A LIQUID-COOLED CONTAINED-ELECTROLYTE LOW-TEMPERATURE

FUEL CELL SYSTEM OVER A PERIOD OF 1500 HOURS

by J. M. McKee, N. H. Hagedorn, and R. W. Easter

Lewis Research Center
National Aeronautics and Space Administration
Cleveland, Ohio

ABSTRACT

A 1500-hour performance investigation was conducted on a 2 kW liquid-cooled contained-electrolyte low-temperature ($\sim 165^{\circ}\text{F}$) fuel cell system. Average cell potential loss at the 2kW level was 31 microvolts per hour. Short-term overloads to 3.5 kW had no permanent effect on subsequent performance, and there was no apparent change over the test duration in the system's ability to handle brief overloads. Bootstrap restart capability at room temperature was demonstrated.

After 1500 hours on load the fuel cell stack was flushed with fresh electrolyte and put back on test for 50 hours. Performance approached the highest level obtained when the stack was new, indicating that the degradation was not a result of any substantial change in the electrochemical characteristics of the cells.

Performance instabilities encountered were primarily attributed to malfunction of systems components and/or corrosion of materials by the electrolyte.

INTRODUCTION

The application of fuel cell power systems to post-Apollo space missions is contingent upon achieving improved performance and endurance over that realized in present qualified hardware. Longer mission times dictate a significant reduction in the time-dependent power degradation of the fuel cell and an improved life for the system's auxiliaries.

A 2kW fuel cell system, the PC8A, purchased from Pratt & Whitney Aircraft Co., was tested at Lewis Research Center for 1500 hours during the last half of 1967 in order to investigate the time related effects of operation under typical NASA test profiles. The PC8A operates at a nominal temperature of 165°F and differs from other contained electrolyte cell stacks in that the major portion of the reaction heat is removed by a circulated liquid coolant.

Investigation of power loss as a function of time under typical mission power profiles was emphasized. The interaction of the fuel cell stack and the system's

components was also of interest, but, since these auxiliaries were of standard commercial grade, a reliability evaluation was not an objective.

FUEL CELL DESCRIPTION

The fuel cell stack is composed of 36 single cells connected in series. Each cell consists of an integral anode and cathode separated by a 10-mil asbestos matrix containing the aqueous KOH electrolyte ($\sim 35\text{ wt } \%$) and sealed in a gasket-frame as shown in Fig. 1. The anode is a 30-mil sintered-nickel plaque with 20 mg/cm^2 of mixed platinum and palladium as the catalyst. The 6-mil cathode contains 10 mg/cm^2 of platinum-palladium catalyst, PTFE-bonded to a fine-mesh gold-plated nickel screen.

Bipolar backup plates are inserted between adjacent cells in order to form cavities for the reactant gases and to provide an inter-cell current path. These hollow plates are electro-etched from magnesium and then silver plated for protection against electrolyte corrosion and for good electrical contact with the cell. Both the fluorocarbon coolant, which flows through these hollow plates, and the fuel cell reactants are manifolded to the individual cells and metered by orifices in the separator plates. Figure 2 shows the fuel cell stack mounted in the PC8A system.

A reactant- and coolant-flow schematic is shown in Fig. 3. Hydrogen and oxygen are supplied to the system at 75 psig and 70°F , reduced to 3 ± 0.5 psig by the input regulators, and distributed to the individual cells through the stack manifolds.

In the oxygen system, a recycle venturi partially humidifies the incoming gas in order to alleviate drying of the cell matrix at the inlet ports. With the 99.5 percent-pure oxygen used in this test, it was necessary to vent continuously, thus limiting the effectiveness of the venturi. With the 99.995 percent-pure oxygen specified for flight systems, the inlet drying that did occur might have been prevented.

The hydrogen system is more complex. Product water is removed from the cell by circulating comparatively-dry excess hydrogen through the anode cavity. Make-up gas enters the flow stream of hydrogen and

TM X-52455

water vapor leaving the module. The combined flow enters the condenser where it is cooled and a portion of the water vapor is condensed and separated. A vane type hydrogen pump maintains the required flow rate.

The amount of water picked up by the hydrogen stream is a function of the incoming-gas humidity, the electrolyte concentration, and the temperatures of the gas and the cell. The water content of the incoming stream is determined by the condenser-outlet temperature, and that leaving is a function of the electrolyte concentration and of temperature at the cell exit. The temperatures of the coolant entering the module and the hydrogen leaving the condenser are maintained at prescribed levels by proportioning the coolant flow through the heater, heat exchanger, and by-pass. The coolant temperature at the cell exit depends on the coolant flow rate and the heat generated by the reaction. Over the design power range, the water removal rate is self-regulating; at high power levels, the coolant ΔT across the cell is great, resulting in a large difference between inlet and outlet humidities and rapid water removal. Conversely, at low power levels, for which water-production rate is less, water removal is diminished.

The coolant heater provides heat for startup and maintains fuel cell temperature when the reaction heat is insufficient. Two servo-driven proportioning valves divide the flow between the heater, heat exchanger, and by-pass in order to maintain the module-inlet coolant temperature at $145 \pm 2^\circ \text{F}$ and the condenser-outlet hydrogen temperature at $119 \pm 2^\circ \text{F}$. These control temperatures may be varied over a narrow range by adjustment of the servo amplifier.

TEST DESCRIPTION

The 1500-hour test consisted of three major segments:

(1) The initial 280 hours consisted of five performance-mapping power profiles suggested by the NASA Manned Spacecraft Center and included short-duration power overloads and bootstrap startup from room temperature. Two 48 hour test cycles were run each week.

(2) From hour 280 to hour 1130, a 24-hour cyclic power profile was followed. During this portion of the program, tests were suspended over weekends. Five power-overload steps were programmed each 100 hours.

(3) The following 370 hours were run continuously except for brief interruptions dictated by operational difficulties. With completion of 1500 hours on load, the fuel cell stack was flushed and refilled with fresh electrolyte and then put on test for an additional fifty hours.

A digital data system hourly recorded all steady-state data. Recorded data included: module voltage and current, single-cell voltages, reactant flow rates to the module, coolant flow rates in all legs of the coolant loop, reactant and coolant pressures, reactant pressure drops across the module, and the hydrogen pressure drops

across the pump and the condenser. A total of 17 temperatures in the module and in the reactant-and coolant-flow channels were measured by means of a null-balance potentiometer. Transient data were recorded either on an 8-channel strip-chart recorder or a light-beam-galvanometer recorder, depending on the frequency response required.

RESULTS AND DISCUSSION

Performance Mapping Tests

The first three test profiles (Fig. 4) were designed to demonstrate fuel cell performance at loads up to 2500 watts for periods of from 3 to 12 hours at each level. Figure 5(a) shows the steady-state module potential obtained at each power plateau for these first three profiles. Figure 5(b) presents the average cell potential (volts) as a function of current density (amperes per square foot) for the same period. The dashed lines indicate the potential spread between the highest and lowest cells in the stack.

Transient Response To Overloads

The response of the fuel cell power output to step changes in load was investigated in power profiles 4 and 5 (Fig. 6), and A (Fig. 9).

In general, the load power was stepped up to some value equal to or in excess of the system's rating of 2kW, held there for a period of time, and then returned to the initial level. In no case did the subsequent final steady-state performance vary from the initial steady-state performance.

The characteristics of the load used were such that the current increase was very nearly a step function (Fig. 7). The stack voltage instantaneously decreased about 60 to 80 percent of the total final change, and then continued to drop until it was below the eventual high-drain steady-state level. A voltage minimum was reached after 15 to 25 sec, and the voltage then gradually rose to the high-drain steady-state value within 3 to 4 minutes.

The initial voltage loss may be attributed to increased resistive voltage drops within the cells and the remaining transient behavior, at least qualitatively, to the establishment of new temperature- and electrolyte-concentration gradients within the cells.

Over the 1100 hours during which short-duration power overloads were introduced, the overload steady-state voltage could be predicted by extrapolating the polarization curve exhibited during operation at normal power levels, the slope of which varied from -45 mV/amp at 300 hours to -60 mV/amp at 1000 hours.

Bootstrap Startup

This test demonstrated the system's restart cap-

ability by "boot-strapping" it to operating condition from room temperature with fuel cell power energizing both the heater and pump circuits. To simplify operation, the required power was actually supplied from an external source and an equivalent amount from the fuel cell dissipated in the load bank. At a fuel-cell potential of 30 volts, the heaters consume 11 amperes and the hydrogen and coolant pumps a little over 4 amperes each; thus any current over 20 amperes represents usable power generated during startup.

Four bootstrap starts were performed at currents of 12, 20, 30, and 40 amperes. Note that the 12-ampere case is strictly academic as this is 8 amperes less than the minimum requirement. Figure 7 presents the time required to reach operating temperature (coolant into module = 145° F) as a function of current drawn from the fuel cell stack. It is recognized that higher loads appreciably shorten the time requirement.

Since the PC8A system was not designed for power production below normal operating temperature, the bootstrap startups resulted in severe cell wetting and electrolyte dilution. Normally the coolant-flow controllers maintain the temperature of the hydrogen leaving the condenser and the coolant into the module stack at levels required to keep the electrolyte concentration at approximately 35 percent KOH by weight. Figure 8 shows that, depending on the fuel-cell load, the system operated outside the control range for a period of from 20 to 45 minutes during which more water was being produced than was being removed. Droplets of electrolyte were entrained in the recirculating hydrogen stream and removed with the product water in the condenser-separator. This resulted in a reduction of OH-ion content in the cells.

For an application requiring numerous restarts, modification of the control system would be required.

Life Performance Evaluation

The remaining 1220 hours of test were conducted on the cyclic power profiles shown in Fig. 9.

Figure 10 is a plot of fuel cell voltage at the 1- and 2-kilowatt levels over the 1500 hours of test. The irregularities, which are more pronounced at the 2-kilowatt level, can in part be attributed to component malfunctions as chronologically listed in Table I.

A major cause of performance degradation is improper electrolyte water balance. If water removal is less than the production rate, the electrolyte will be diluted, and, in the extreme, the electrode will be partially flooded and the fuel gas prevented from reaching the reaction sites. If excess water is removed, the electrolyte volume will be diminished, and eventually the matrix-electrode interface area will be reduced. Furthermore, insufficient moisture in the matrix tends to allow drying in the area of the inlet oxygen port. (The oxygen entering the cell was comparatively dry as a result of the

continuous vent required to purge inerts.) Since the bubble pressure of asbestos matrices decreases with decreasing electrolyte content, reactant cross-leakage can result.

Referring again to Fig. 10, the dropoff at 150 to 200 hours was caused by excess water production, i.e., electrolyte dilution, during the power overload tests.

At about 450 hours the coolant heat exchanger developed a leak and was replaced by a coolant coil running through a cold bath. This change in flow path caused an unbalance in flow pressure drops through the coolant loops and resulted in oscillation of the hydrogen- and coolant-temperature controllers. A needle valve was placed in the coolant line and adjusted periodically over the following 100 hours in order to reestablish control at all profile power levels.

An obstruction in the coolant exit manifold from the front half of the stack (cells 1-18) developed at about 700 hours. This made it impossible to remove equal amounts of heat from both halves of the stack, and hence a stable electrolyte-water balance was impossible. From this time forward the hydrogen inlet humidity was adjusted to provide for the most favorable overall electrolyte balance as indicated by the individual cell performances.

The performance dip at 1000 hours resulted from reactant cross-leakage in several cells. This was indicated by poor performance of the cells and confirmed by detection of hydrogen in oxygen vent. From hour 1000 to hour 1500, it was occasionally necessary to interrupt operation for short periods of time (20 minutes to 2 hours) to allow the electrolyte to redistribute in the matrix, to reestablish the electrolyte-electrode interface, and to eliminate cross leaks. Three cells (Nos. 3, 6, and 28) showed evidence of cross leakage.

During the next 370 hours, scheduled continuous operation was interrupted twelve times for a total of 16 hours because of apparent cross leaks.

Following the test, tear down analysis indicated some corrosion of the silver layer of the bipolar plates had occurred.

In general, each problem encountered could be classified in one of the following categories:

- (1) Failure of coolant system to provide adequate, uniform heat removal.
- (2) Catastrophic failure of auxiliary components (i.e., other than fuel cell stack).
- (3) Presence of materials subject to corrosive attack by the electrolyte.
- (4) Effects of off-design operation.

With few exceptions, these problems were manifested by an adverse effect on cell electrolyte volume and concentration, and it was this recurrence of unfavorable

electrolyte balance conditions that primarily dictated the performance and degradation characteristics of the system.

In spite of the problems enumerated, the performance of the fuel cell stack, particularly with respect to voltage degradation, compared favorably with the present state of the art. Figure 11 is a plot of module voltage against power output at 50, 500, 1000, and 1500 hours. Figure 12 shows the average single-cell voltage loss (microvolts per hour) against load current (amperes) over the 1500-hour period. The data indicate that performance of five cells (numbers 2, 3, 4, 5, and 6) fell at a significantly higher rate than the others as indicated by the top curve, possibly because of the coolant flow imbalance. The minimum in the degradation curve between 20 and 40 amperes is attributed to the relative thermal stability of the fuel-cell stack in that range. Below 20 amperes the coolant heaters were cycling on and off, and above 40 amperes the temperature difference across the cell increased appreciably.

Post-Test Evaluation

After the 1500-hour test, the fuel cell stack was removed from the system, flushed out, and refilled with fresh electrolyte. The module was put on test, repeating performance mapping profile No. 1. After 30 hours, the fuel cell equilibrated at the same performance level as the 0 to 50-hour profile shown in Fig. 11. Most cells were running very close to their original performance level; a few were better and a few worse. Open-circuit potentials indicated low-current short circuits in 5 cells. A subsequent tear-down analysis of the cell matrices showed evidence of cross leakage as indicated by dry, discolored spots in several cells.

CONCLUSIONS

The 1500-hour evaluation demonstrated that the PC8 system concept can lead to a practical power source for post-Apollo space applications.

The fuel cell itself demonstrated a moderate and acceptable degradation rate for the 1500-hour period. Short-duration overloads up to 175 percent of rated power had no permanent effect on subsequent performance. There was no apparent change over the test duration in the system's ability to handle brief overloads.

The "irregularities" in fuel cell performance encountered during the testing could in all cases be related to materials or system component and control problems; i. e., the electrochemical characteristics of the cells, in particular the electrode catalyst activity, apparently did not contribute to performance degradation.

TABLE I. - OPERATIONAL PROBLEMS ENCOUNTERED
DURING 1500 HOUR FUEL CELL TEST

Cumulative hours	Malfunction
82	H ₂ pump vane failure; replaced it and coolant pump.
290	Heat exchanger fouled; cleaned and replaced.
426	Heat exchanger fouled; cleaned and replaced. Leaked on replacement. Substituted copper tubing coil in coolant bath.
495	Coolant control unbalanced. Cells 1 to 14 performance falling off. Adjustment valve put in coolant loop for balance.
599	Replaced gate valve in coolant loop with needle valve for finer control.
620	Noted coolant unbalance between front and rear halves of the module.
922	Reactant gas cross leakage verified by hydrogen-oxygen analyzer. O ₂ inlet and outlets switched.

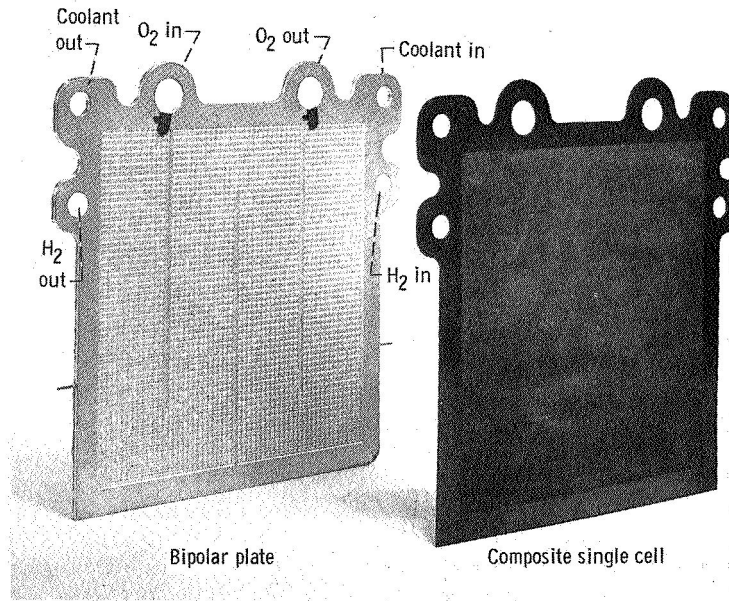
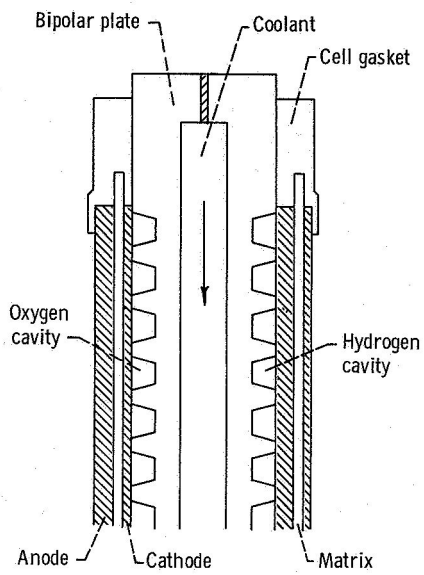


Figure 1. - Single unitized cell, bipolar plate.

C-68-1391

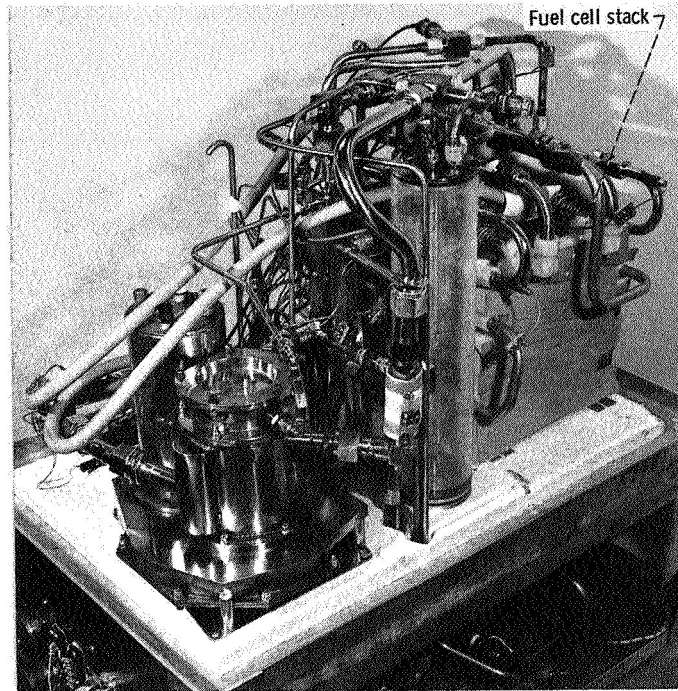


Figure 2. - PC8A System photograph. Reprinted by courtesy of Pratt and Whitney Aircraft.

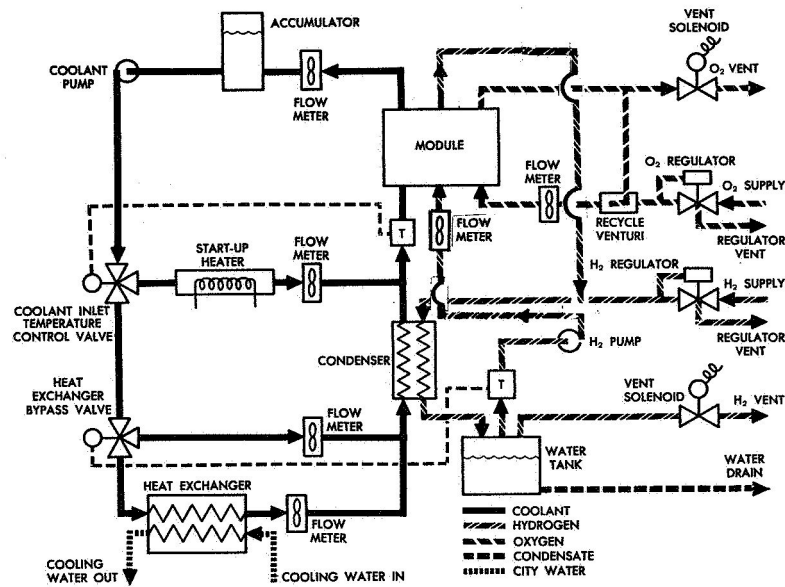


Figure 3. - PC8A system schematic. Reprinted by courtesy of Pratt and Whitney Aircraft.

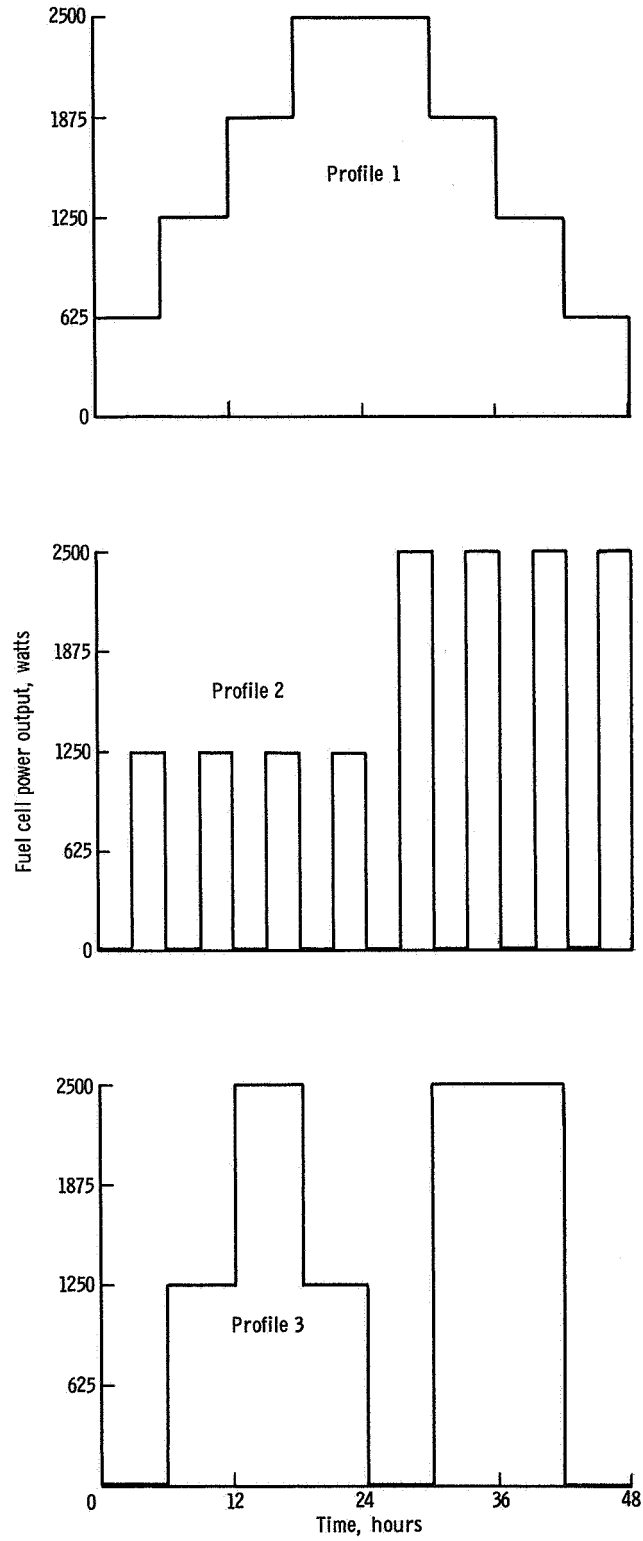


Figure 4. - Performance mapping test profiles.

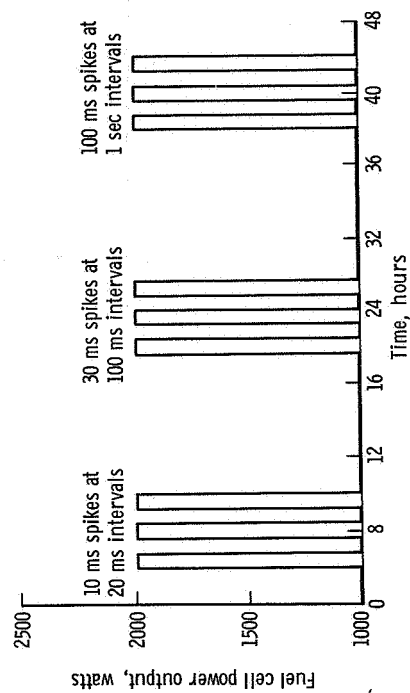
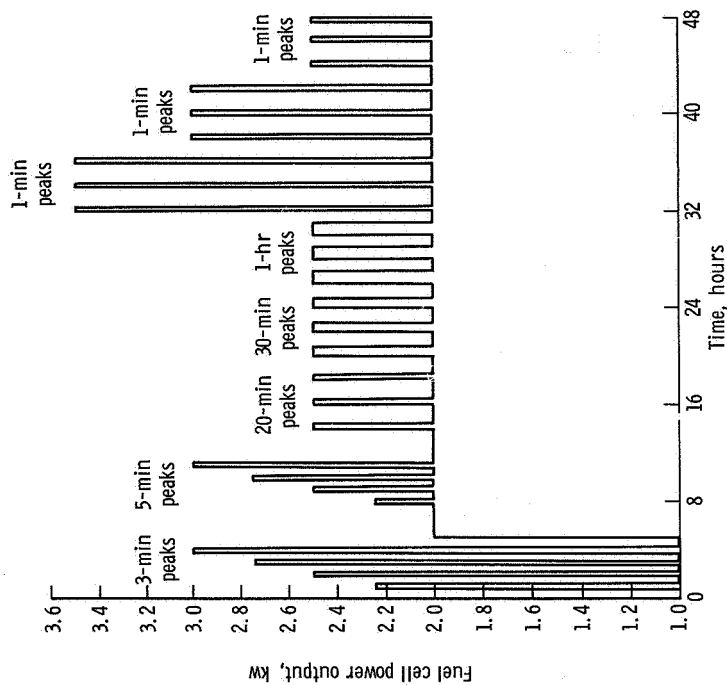
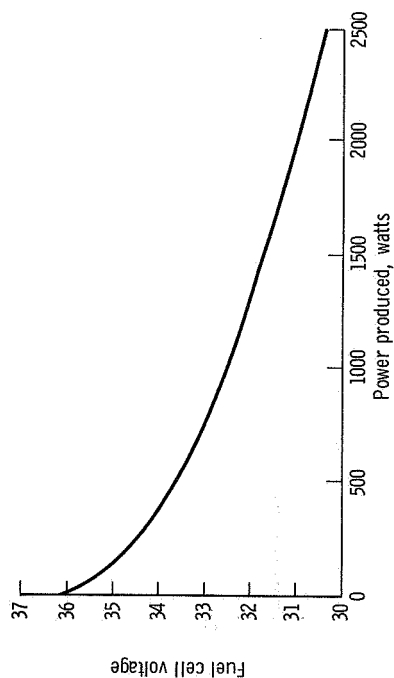
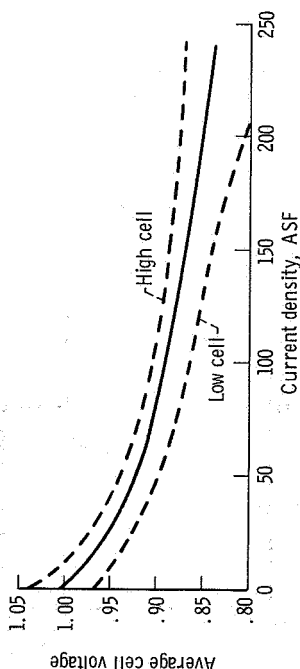


Figure 6. - Overload power profiles.



(a) Fuel cell stack voltage versus gross power.



(b) Average cell voltage versus current density.

Figure 5. - Fuel cell performance, 0 to 144 hours.

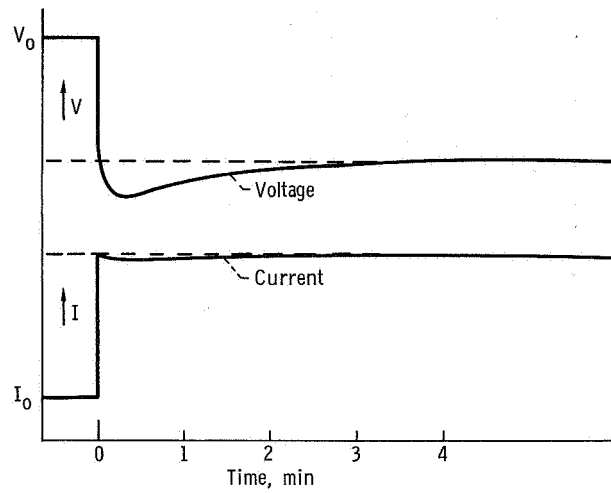


Figure 7. - Overload response.

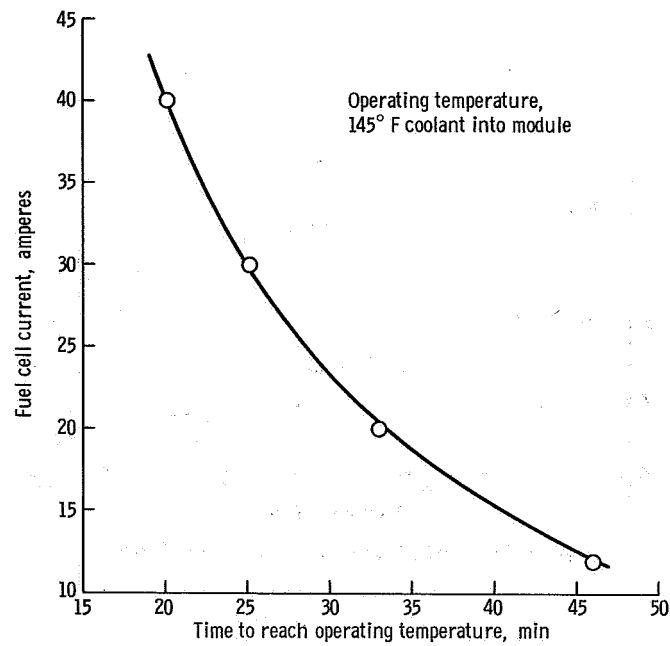
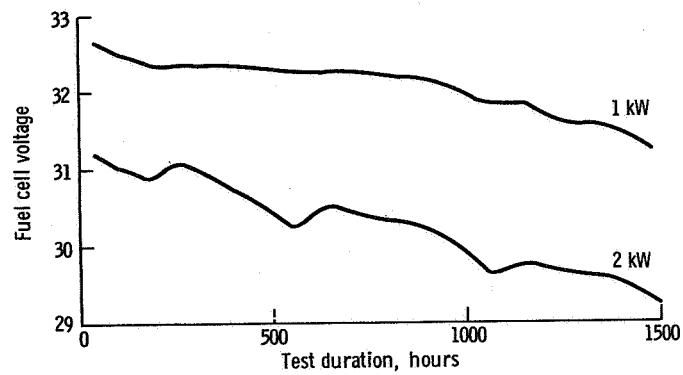
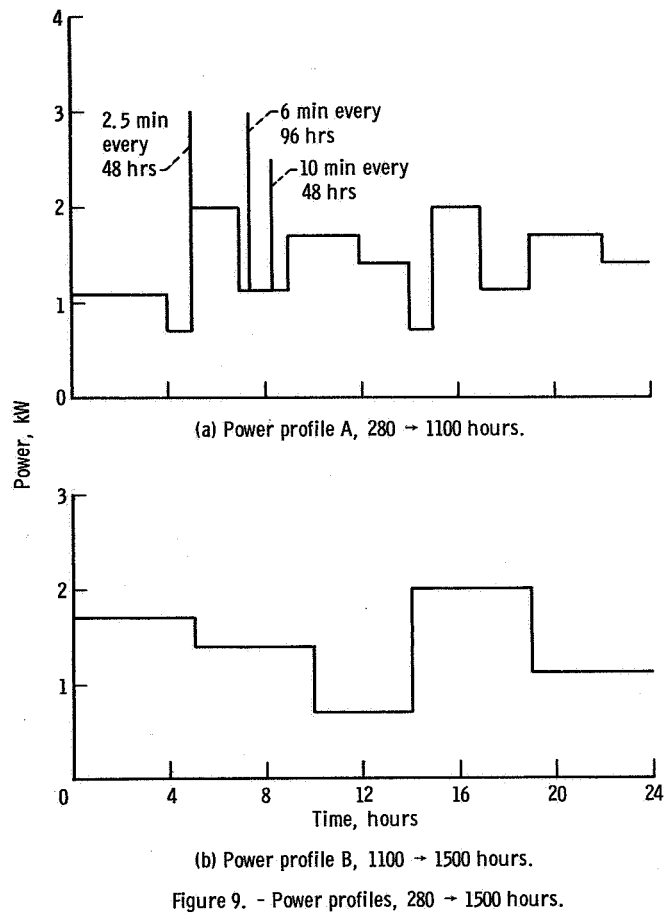


Figure 8. - Bootstrap startup.



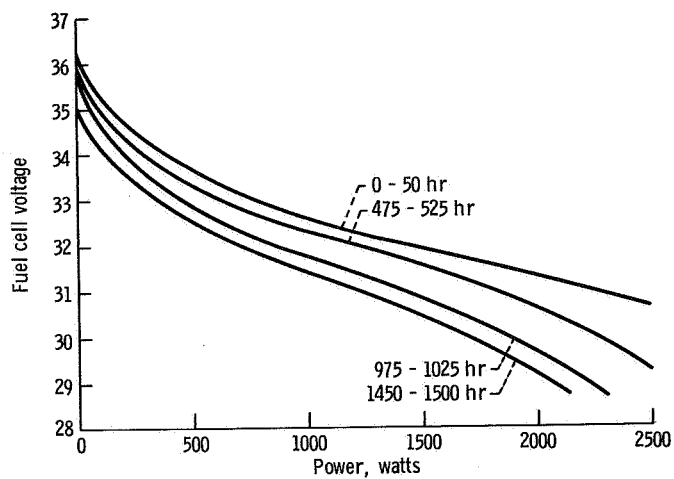


Figure 11. - Power density, 0 - 1500 hours.

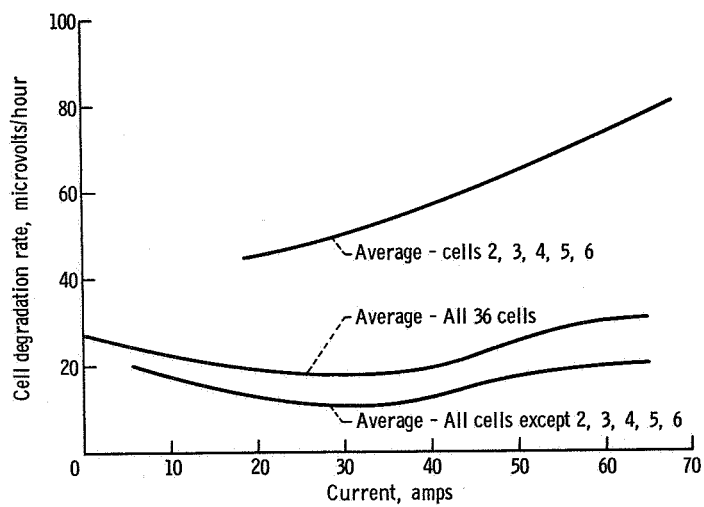


Figure 12. - Average cell degradation versus load current.